Journal of Materials Chemistry A

Accepted Manuscript

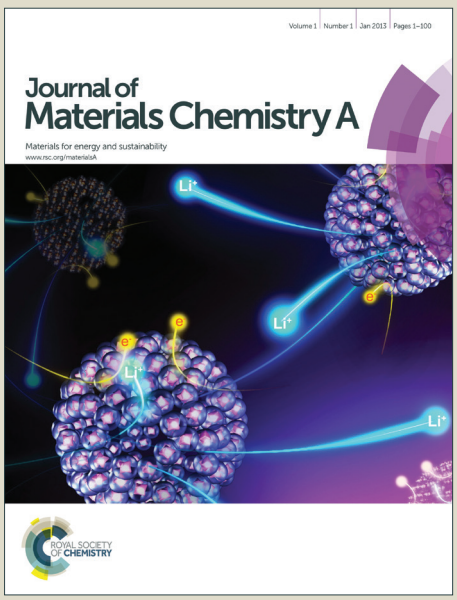

ROYAL SOCIETY OF CHEMISTRY

www.rsc.org/materialsA

Journal of Materials Chemistry A

Cite this: DOI: 10.1039/c0xx00000x

www.rsc.org/xxxxxx

COMMUNICATION

RuO_2/rutile-TiO_2: A Superior Catalyst for N_2O Decomposition

Qingquan Lin,[a,b,c] Yanqiang Huang,*[b] Yong Wang,[d] Lin Li,[b] Xiao Yan Liu,[b] Fei Lv,[b] Aiqin Wang,[b] Wen-Cui Li[a] and Tao Zhang[b]

Received (in XXX, XXX) Xth XXXXXXXXX 20XX, Accepted Xth XXXXXXXXX 20XX
DOI: 10.1039/b000000x

A newly developed RuO_2/rutile-TiO_2 catalyst displays a remarkable activity and stability in N_2O decomposition. The outstanding performance was attributed to the formation of uniformly coated RuO_2 thin film on rutile-TiO_2.

Nitrous oxide (N_2O), a widespread greenhouse gas, can also be used as a green propellant [1]. Over the last decades, considerable efforts [2] are currently underway to develop efficient catalysts to decompose N_2O due to its significance in environmental catalysis and chemical propulsion. Ruthenium dioxide (RuO_2) has long been recognized as an efficient catalyst towards N-O bond dissociation and thus renders a promising candidate for N_2O decomposition [3]. However, RuO_2 nanoparticles are easily aggregated in oxidative atmosphere [4] due to the volatility of oxidized ruthenium, which eventually restricted their catalytic applications in N_2O decomposition since high concentration of O_2 is evolved as a product in this reaction. Many attempts were consequently made to stabilize RuO_2, and its stabilization in the crystal structure of heat-resistant materials, such as hexaluminate [4] and perovskite [5], received much attention. However, most of the ruthenium species were buried in these bulk materials, and thus the obtained catalysts were only active at temperatures above 400 °C. Therefore, current research concentrates on searching for a suitable oxide support to stabilize RuO_2 through strong oxide-support interaction (SOSI).

Titania (TiO_2) has been one of the preferred SOSI supports, over which it usually led to the formation of monolayer of active phases (e.g. VO_x, CrO_x). Previous reports showed that RuO_2, if deposited on the surfaces of TiO_2, exhibited desired activity and stability in catalytic HCl oxidation ($4HCl+O_2=2H_2O+2Cl_2$) [6]. Such acquired catalytic performance was due to the formation of epitaxial RuO_2 monolayer over the surface of TiO_2. To be noted, the morphologies of RuO_2 depended on the crystal structure of the TiO_2, and the RuO_2 monolayer can be generated only on the rutile-type TiO_2 as the RuO_2 phase possesses the same rutile structure. However, no studies have so far been performed on RuO_2/TiO_2 for N_2O decomposition, in spite of that TiO_2 can efficiently stabilize RuO_2 under oxidizing conditions. This is probably due to the fact that previous catalysts based on redox oxide supports, such as CeO_2 and TiO_2, showed moderate activities in N_2O decomposition [2e]. Herein, we present a novel catalyst for N_2O decomposition by depositing RuO_2 on rutile-TiO_2 support, which exhibited a surprisingly high activity and stability.

In this communication, TiO_2 with different crystalline phases were prepared by controllable phase transition via wet-chemical route [7], and the synthesis details were described in supporting information (SI). The analysis of XRD patterns (Fig. S1a, PDF No. 04-0551 and 21-1276) and raman spectroscopy (Fig. S1b) confirmed that the TiO_2 supports were phase-pure rutile and anatase as desired. The specific surface area of rutile-TiO_2 and anatase-TiO_2 (shorted as r-TiO_2 and a-TiO_2, respectively) is 27 and 45 m^2g^{-1}, respectively. Crystalline size and porosity of these supports were shown in Table 1. RuO_2 species were deposited on the supports by wet-impregnation method. Prior to catalyst testing, the RuO_2/TiO_2 was pre-treated in air at 300 °C for 4 h to activate the catalyst.

Figure 1a shows the N_2O conversion as a function of reaction temperature of RuO_2 nano-particles loaded on several supports. The RuO_2/r-TiO_2 catalyst exhibited a surprisingly high activity and the onset temperature of catalytic N_2O decomposition was as low as 180 °C, which is much lower than that reported on the supported iridium (300 °C)[2c] and rhodium (250 °C) [2d] catalysts. Considering the different curves in Fig.1, a significant support effect is observed. The RuO_2/r-TiO_2 catalysts exhibited the highest N_2O conversion, compared with those RuO_2 catalysts by using a-TiO_2, Al_2O_3, and SiO_2 as a support. In order to further explore the intrinsic catalytic activity, the specific rates of the investigated catalysts at 220 °C were also calculated (Table 1). The reaction rate over present RuO_2/r-TiO_2 catalyst was calculated to be 2.30 mol_{N2O} min^{-1} mol_{RuO2}^{-1}, much higher than the results of RuO_2 catalysts supported on a-TiO_2 (0.77), Al_2O_3 (0.18), SiO_2 (0.20), implying that r-TiO_2 is a better support to

[a] *State Key Laboratory of Fine Chemicals, School of Chemical engineering, Dalian University of Technology, Dalian 116024, China.*
[b] *State Key Laboratory of Catalysis, Dalian Institute of Chemical Physics, Chinese Academy of Sciences, Dalian 116023, China. Fax: (+) 86 411 84685940 E-mail: yqhuang@dicp.ac.cn (Y. Huang)*
[c] *Graduate University of Chinese Academy of Sciences, Beijing 10049, China.*
[d] *Center of Electron Microscopy and State Key Laboratory of Silicon Materials, Department of Materials Science and Engineering, Zhejiang University, Hangzhou 310027, China.*
† *Electronic Supplementary Information (ESI) available: details of catalyst preparation, reaction measurement, as well as characterization data of XRD, HAADF-STEM, XPS. See DOI: 10.1039/b000000x/*

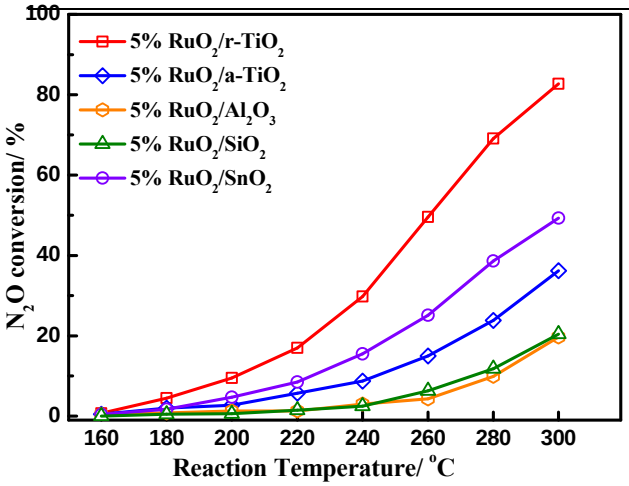

Fig. 1 N_2O conversions as a function of the reaction temperature for various RuO_2 catalysts

Reaction conditions: 30 vol% N_2O balanced with Ar. Weight hourly space velocity (WHSV): 30,000 mL g_{cat}^{-1} h^{-1}.

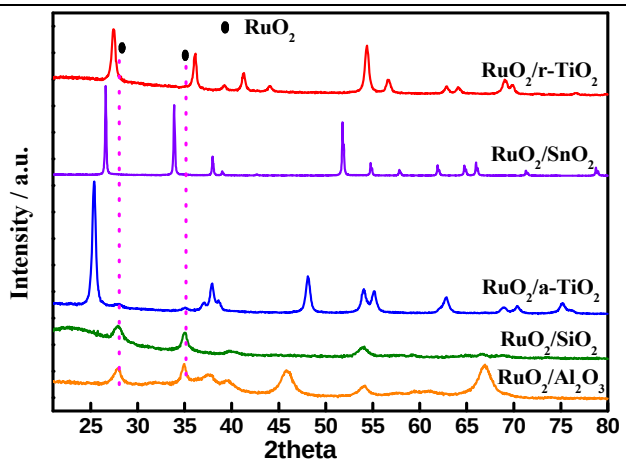

Fig. 2 The XRD patterns of various RuO_2 catalysts

load RuO_2 for N_2O decomposition. The more striking observation is that the reaction rate of RuO_2/r-TiO_2 was three times as high as that of RuO_2/a-TiO_2, in spite of the lower surface area of r-TiO_2. The results indicated that, in the case of using TiO_2 as a support, the phase matters: r-TiO_2 is preferred to a-TiO_2. To confirm this point, the rutile-type oxide SnO_2 supported RuO_2 catalyst was investigated in this reaction and also exhibited a much higher activity than the RuO_2/a-TiO_2 catalyst, indicating that the rutile-type oxide was a superior support for RuO_2 catalysts in the reaction of N_2O decomposition. Additionally, we tested the stability of the RuO_2/r-TiO_2 in N_2O decomposition at 300 °C for more than 60 hs (Fig. S2). Minor activity loss was only observed at the beginning of the test and then the N_2O conversion reached a plateau. Furthermore, using r-TiO_2 as the catalyst support, we also investigated the effect of RuO_2 loading on catalytic activity. As it has been reported by Kawi et al.[3c], the catalyst activity increased as the Ru loading increased from 0.2 to 5.0 wt% (Fig. S3a). The maximum specific rate was observed in this study at the Ru loading of 0.2 wt% (Fig. S3b).

To reveal the unique properties of RuO_2/r-TiO_2 in N_2O decomposition, further studies were performed to discuss the influence of the support on the structure of the RuO_2 active phases. As the XRD profiles presented in Fig. 2, there were no diffraction peaks of RuO_2 observed if they were deposited on the oxides with the rutile structure, such as r-TiO_2, SnO_2, indicating a high dispersion of RuO_2. However, on other standard supports, such as a-TiO_2, SiO_2, Al_2O_3, two diffraction peaks corresponding to RuO_2 were clearly observed indicating the aggregation of RuO_2, and their calculated average crystalline sizes of RuO_2 were all beyond 10 nm (Table 1). This point can be verified from the HAADF-STEM images. Severely sintered nano-particles of ruthenium oxides larger than 10 nm, in the shape of bright round spot or narrow strip, were found on the surface of a-TiO_2 (Fig. S4b), and the aggregation of RuO_2 became more severely if deposited on SiO_2 and Al_2O_3 support (Fig. S4c, S4d). To be noted, a few small RuO_2 nanoparticles were also revealed in the images with high magnification (Fig. S5b-d). But we could not find any visible RuO_2 nanoparticles for RuO_2/r-TiO_2 catalyst despite of our careful observation (Fig. S4a, S5a), indicating a high dispersion of RuO_2 species. Moreover, sintering of RuO_2 was prevented when rutile-SnO_2 is used as the support (Fig. S4e, S5e). These results demonstrated that oxide supports with rutile structure can stabilize RuO_2 species under oxidative conditions.

We further focused on the structural characterization of RuO_2/a-TiO_2 and RuO_2/r-TiO_2 through high-resolution transmission electron microscopy (Fig. 3). The result displayed that the RuO_2 species appears on the surface of r-TiO_2 in the form of thin film, while RuO_2 on a-TiO_2 features a cubic nanoparticles. This phenomenon could be explained by the high degree of the interfacial lattice matching between RuO_2 and rutile-TiO_2/SnO_2 because they were both the same rutile-type oxide and had nearly the same lattice parameters

Table 1 Characterization and catalytic data of various RuO_2 catalysts

Catalysts	The support information		Ru loading (wt %)	Crystalline size (nm)	Conversions (%) of 30% N_2O at 220 °C	Reaction rate at 220 °C (mol_{N2O} min^{-1} mol_{Ru}^{-1})
	S_{BET} (m^2 g^{-1})	Porosity (mL g^{-1}) & Crystalline size (nm)				
RuO_2/r-TiO_2	27	0.13 / 15	5.0	ud	17.0	2.30
RuO_2/a-TiO_2	45	0.15 / 21	5.0	10.7	5.7	0.77
RuO_2/Al_2O_3	273	——	5.0	12.2	1.3	0.18
RuO_2/SiO_2	384	——	5.0	14.1	1.5	0.20
RuO_2/SnO_2	5	——	5.0	ud	8.5	1.15

Note: ud means undetected.

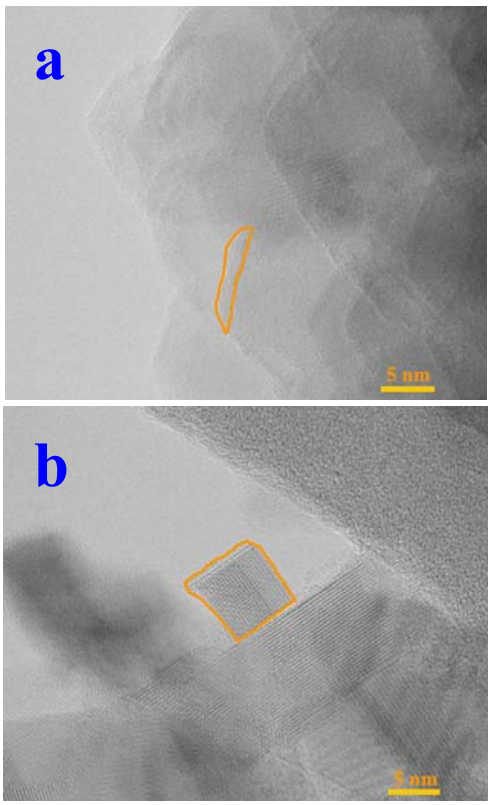

Fig. 3 HRTEM images of supported RuO_2 catalysts
(a) RuO_2/r-TiO_2 and (b) RuO_2/a-TiO_2

(a=b=4.49 Å, c=3.11 Å for RuO_2, a=b=4.59 Å, c=2.96 Å for r-TiO_2 and a=b=4.75 Å, c=3.19 Å for SnO_2). An intimate interaction will occur between RuO_2 and oxides with rutile structure due to their high degree of lattice matching, which in turn stabilizes the RuO_2 under oxidation conditions and maintains its high dispersion. But for a-TiO_2, SiO_2, Al_2O_3, the degree of lattice mismatch with RuO_2 was quite high (a=b=3.78 Å, c=9.51 Å for a-TiO_2, a=b=c=7.94 Å for Al_2O_3 and a=b=4.91 Å, c=5.40 Å for SiO_2), and thus loosing the ability to stabilize RuO_2.

The intimate contact between RuO_2 and r-TiO_2 was further confirmed by Raman spectroscopy (Fig. 4). The typical Raman bands due to r-TiO_2 appear at 446 and 612 cm^{-1}, which can be ascribed to the E_g (planar O-O vibration) and A_{1g} (Ti-O stretch) modes of rutile phase, respectively. Depositing RuO_2 species on r-TiO_2 surface induced a red shift of E_g mode by ca. 17.6 cm^{-1} while the A_{1g} mode did not shift at all. The observed frequency shift is consistent with the results reported by Siegel and Swamy [8], indicating the modification of the planar O-O vibration. The obvious reason is that r-TiO_2 can accommodate RuO_2 within its structure. The growth of RuO_2 with the same orientation as r-TiO_2 is accompanied by the formation of Ru-O-Ti bond. This interaction has a more significant effect on the planar O-O vibration (446 cm^{-1}) than the Ti-O stretch (612 cm^{-1}). Besides, the E_g mode of RuO_2 was observed at 508 cm^{-1} indicating its existence in the catalyst. In contrast, after depositing RuO_2 on the surface of a-TiO_2, there were no changes of the three dominant Raman-active modes of the configuration, E_g, A_{1g}, B_{1g} located at 638, 514 and 397 cm^{-1}, respectively. Moreover, X-ray photoelectron studies of (Fig. S6) RuO_2/r-TiO_2 showed that

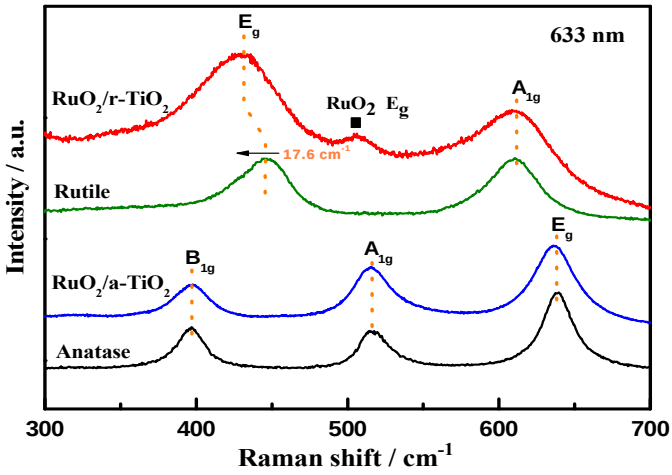

Fig. 4 Raman spectra of various materials (λ_{max}=633 nm)

the Ru 3d spectrum displayed a shift of 0.2 eV towards higher binding energies (B. E.), and the Ti 2p spectrum of r-TiO_2 shifted 0.3 eV towards lower B.E.. The observation indicates a charge transfer [9] from the RuO_2 to r-TiO_2, which is probably caused by the chemical bonding between them.

Over the investigated RuO_2 catalysts, the N_2O decomposition activity agrees well with the RuO_2 dispersion. RuO_2 particle size differs significantly depending on the supports employed, which is the main reason for their activity variation. Owing to the structural similarity with RuO_2, r-TiO_2 support enables the formation of RuO_2 thin film, which can maximize the dispersion of active phase. Moreover, DFT calculation [10] indicated that the specific RuO_2 (110) planes, generated due to the epitaxial growth on r-TiO_2, could make a great contribution to the activity. However, this point still needs further experiment to clarify. Overall, RuO_2/r-TiO_2 exhibited an unexpected high activity and stability in N_2O decomposition. Despite the benefits introduced, further improvement of the thermal stability is still required because of the highly exothermic nature of this reaction.

In conclusion, we reported a highly active and stable catalyst for the N_2O decomposition by depositing RuO_2 on r-TiO_2. The monolayer structure of RuO_2 maximized the metal dispersion, and thus produced a highly active catalyst. Moreover, the intimate contact of RuO_2 with r-TiO_2 improved its stability, producing a durable catalyst.

Notes and references

This work was supported by the NSFC (21103173, 21173218, 51390474 and 21303192).

1 [a] B. Delmon, *Appl. Catal. B*, 1992, **1**, 221; [b] V. Zakirov, M. Sweeting, V. Goeman, T. Lawrence, *Proceedings of the 14th Annual AIAA/USU Conference on Small Satellites*, USA, 21-24 Aug. 2000.

2 [a] J. Pérez-Ramírez, F. Ramirez, G. Kapteijn, J. A. Moulijin, *Appl. Catal. B*, 2003, **44**, 117; [b] J. Pérez-Ramírez and M. Santiago, *Chem. Commun.*, 2007, 619; [c] S. Zhu, X. Wang, A. Wang, Y. Cong, T. Zhang, *Chem. Commun.*, 2007, 1695; [d] X. Zhao, Y. Cong, F. Lv, L. Li, X. Wang, T. Zhang, Chem. Commun., 2010, 3028; [e] H. Beyer, J. Emmerich, K. Chatziapostolou, K. Köhler, *Appl. Catal. A*, 2011, **391**, 411.

3 [a] Y. Chang, J. G. McCarty, E. D. Wachsman, *Appl. Catal. B*, 1995, **6**, 21; [b] F. Pinna, M. Scarpa, G. Strukul, E. Guglielminotti, F. Boccuzzi, M. Manzoli, *J. Catal.*, 2000, **192**, 158; [c] S. Kawi, S. Y. Liu, S. C. Shen, *Catal. Today*, 2001, **68**, 237; [d] G. E. Marnellos, E.

A. Efthimiadis, I. A. Vasalos, *Appl. Catal. B*, 2003, **46**, 523; [e] V. G. Komvokis, G. E. Marnellos, I. A. Vasalos, K. S. Triantafyllidis, *Appl. Catal. B*, 2009, **89**, 627; [f] V. G. Komvokis, M. Marti, A. Delimitis, I. A. Vasalos, K. S. Triantafyllidis, *Appl. Catal. B*, 2011, **103**, 62; [g] M. Santiago, V. A. Kondratenko, E. V. Kondratenko, N. López, J. Pérez-Ramírez, *Appl. Catal. B*, 2011, **110**, 33.

4 Y. Zhang, X. Wang, Y. Zhu, T. Zhang, *Appl. Catal. B*, 2013, **129**, 382.

5 N. K. Labhsetwar, A. Watanabe, T. Mitsuhashi, *Appl. Catal. B*, 2003, **40**, 21.

6 [a] K. Seki, *Catal. Surv. Asia*, 2010, **14**, 168; [b] J. Pérez-Ramírez, C. Mondelli, T. Schmidt, O. Schlüter, A. Wolf, L. Mleczko, T. Dreier, *Energ. Environ. Sci.*, 2011, **4**, 4786 [c] G. Xiang, X. Shi, Y. Wu, J. Zhuang, X. Wang, *Sci. Rep.*, 2012, **2**, 801; [d] E. V. Kondratenko, A. P. Amrute, M.-M. Pohl, N. Steinfeldt, C. Mondelli, J. Pérez-Ramírez, *Catal. Sci. Technol.*, 2013, **3**, 2555.

7 A. Sun, P. Guo, Z. Li, Y. Li, P. Cui, *J. Alloys Compd.*, 2009, **481**, 605.

8 [a] J. C. Parker, R. W. Siegel, *J. Mater. Res.*, 1990, **5**, 1246; [b] V. Swamy, *Rhy. Rev. B*, 2008, **77**, 195414.

9 [a] J. P. S. Badyal, R. M. Lambert, K. Harrison, C. C. A. Riley, J. C. Frost, *J. Catal.*, 1991, **129**, 486; [b] L. Näslund, C. M. Sánchez-Sánchez, Á. S. Ingason, J. Bäckström, E. Herrero, J. Rosen, S. Holmin, *J. Phys. Chem. C*, 2013, **117**, 6126.

10 H. Over, *Science*, 2000, **287**, 1474.